Extreme Mechanics Letters 21 (2018) 57–64

Contents lists available at ScienceDirect

Extreme Mechanics Letters

journal homepage: www.elsevier.com/locate/eml

Functionalisation of metal–polymer-nanocomposites: Chemoelectromechanical coupling and charge carrier transport

Jana Wilmers *, Swantje Bargmann

Chair of Solid Mechanics, University of Wuppertal, Germany

ARTICLE INFO

Article history:
Received 5 September 2017
Received in revised form 15 March 2018
Accepted 15 March 2018
Available online 27 March 2018

Keywords:
Multiphysics
Actuators
Interface effects
Nanocomposites
Charge carrier transport
Electromechanical coupling

ABSTRACT

Electrochemical actuation in nanoporous metals is achieved by impregnation of the material's pore space with a ionic conductor, typically an aqueous electrolyte. These hybrid actuators exhibit fully reversible deformation and mechanical properties that can be controlled by electric signals. Recently, set-ups have been proposed in which the nanoporous metal's surface is additionally coated with a conjugated polymer, resulting in a nanocomposite that exhibits strongly increased actuation strains compared to the pure metal while still retaining the mechanical strength of the metal backbone.

In order to exploit the full potential of these nanocomposite actuators, a detailed understanding of the underlying ion transport mechanisms and means to predict the actuator's response are necessary. We present an interface-extended continuum mechanical model to study actuation in pure nanoporous gold and nanoporous gold–polypyrrole nanocomposites. Simulations predict significantly enhanced actuation strains due to the presence of the polymer phase and show that both, the nanocomposite's structure and the ions' mobilities, greatly affect the actuator's response.

1. Introduction

Nanoporous metals are monolithic materials consisting of an interconnected network of nanoscale metal wires, the so-called ligaments. Their characteristic structure [1] gives them an exceptionally high surface-to-volume ratio which is not only responsible for the unique mechanical properties of the material (compare, e.g., [2,3]), but is also the source of chemoelectromechanically coupled behaviour resulting in electrically induced, fully reversible actuation in nanoporous gold [4]. In response to an applied electric field, the metal develops a surface charge which affects the bonding strength of the surface atoms. Small surface modifications like that are negligible in a bulk material, but on the nanoscale, they are translated into macroscopic deformation of the metal. This results in an effective stiffness that can be controlled by the application of an electric field [5]. Beyond that, the inverse behaviour, i.e., generation of an electric current under mechanical loading, has been found to generate significant electric currents with a charge–load coupling coefficient that surpasses that of high-performance piezoceramics [6].

Nanoporous gold has been studied extensively as a model system but for wide-spread application as low-cost electrochemical actuators, other, less exclusive materials need to be employed. In recent years, numerous nanoporous metals have been developed, most of which are still based on noble metals (e.g., palladium [7,8], silver [9,10]) but increasingly non-noble nanoporous metals (e.g., titanium [11] and nickel [12]) and alloys [13,14] can be reliably synthesised, providing a variety of possible material systems for development of high performance actuators and "smart" materials.

Actuation amplitudes observed in nanoporous metals are small compared to other actuators. This drawback can be mitigated by forming a composite of nanoporous gold with a large-strain polymer actuator such as polypyrrole. In these composites, the gold ligaments are covered with the polymer, resulting in a bi-continuous nanocomposite with significantly increased actuation strains [15,16] due to the presence of the polymer and favourable mechanical properties due to the metal backbone. Electroactivity in conjugated polymers such as polypyrrole is based on ion transport within the polymeric network. While response times are comparatively low due to the slow ion transport in the polymer, large deformations at low required voltages are achievable [17].

The presence of a second, polymeric phase in a nanoporous metal is known to affect its mechanical response by introducing new possible deformation mechanisms [18–20]. Significant effects on the actuation behaviour in addition to the increased actuation strain are expected due to the changes in ion transport behaviour. Hierarchical structures have been proposed to optimise electroactive behaviour as larger pores provide routes for fast ion transport, while nanoscale pores provide the necessary high surface area for

* Corresponding author.
E-mail address: wilmers@uni-wuppertal.de (J. Wilmers).

https://doi.org/10.1016/j.eml.2018.03.002

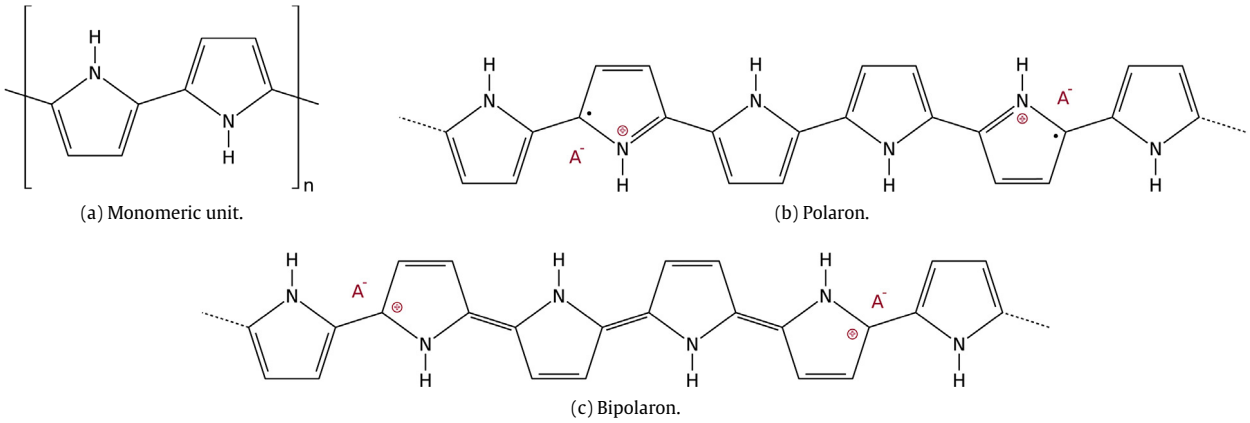

Fig. 1. Polypyrrole (PPy) is a conjugated polymer that can be made electrically conducting through polymer doping. In the doped (oxidised) state, (a) polarons and (b) bipolarons act as charge carriers. Due to the conjugated structure of the polymer chain, polarons and bipolarons are spread out (delocalised) over three or four monomeric units and can be transported along the chain as well as via inter-chain hopping, cf. [31]. The dopant A^- in the sketch balances the polarons' and bipolarons' charge.

actuation [21,22]. Furthermore, actuation in polypyrrole and other conjugated polymers strongly depends on the mobilities of the ions, to the extent that with different ions the same applied potential can result in either shrinking or expansion of the polymer [17].

Computational modelling of the nanocomposite actuator provides the means to study such effects and offers insights into the material behaviour that are inaccessible to experiments, such as the nature of the superposition of the metal's and the polymer's actuation behaviour and the mechanisms involved in ion transport. Modelling of bulk composite actuators has received considerable attention in the past, especially for ionomeric polymer/metal composites, so-called IPMCs [23–25]. The complex charge transport behaviour in conjugated polymers is modelled in [26] without consideration of electromechanical effects. Models for actuation strains and volume changes in conjugated polymers are proposed in [27,28].

None of these available modelling approaches can provide an all-encompassing description of electroactive polymer/metal composites as their behaviour tends to be a superposition of different mechanisms that is not fully understood as of yet. In the following, we focus on modelling effects arising due to the nanoscale nature of the nanoporous gold–polypyrrole composite as studied by [16]. To account for the high interface-to-volume ratio in the nanocomposite and its role in actuation, we adapt the continuum mechanical modelling framework for the chemoelectromechanical coupling in metal–polymer nanocomposites developed in Wilmers et al. [29] to the case of conjugated polymers and use it to study the effect the presence of the polymer phase has on the material's actuation behaviour.[1]

2. Working principle of nanocomposite actuator

The electroactive nanocomposite studied here is based on (partial) infiltration of the metal's pore network with polypyrrole. Both individual constituents of the composite exhibit actuation but the underlying mechanisms are very different. While in nanoporous metals, actuation is a pure interface effect [4], polypyrrole exhibits deformation due to ion insertion into the polymer network.

Conjugated polymers such as polypyrrole are organic semiconductors, that is they can be made electrically conducting by doping with anions, i.e., negatively charged ions. In the doped or oxidised state, the polymer exhibits positive charges along the chains, forming so-called polarons and bipolarons [31] which facilitate electric conduction, compare Fig. 1. The doping anion is incorporated into the polymer network and balances the charge.

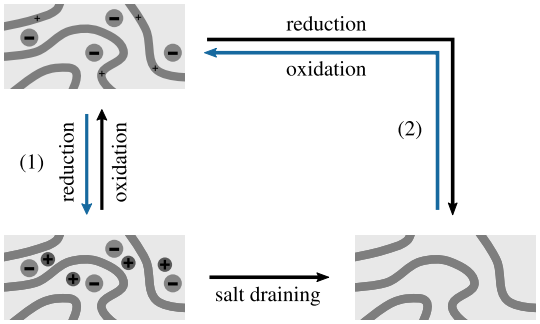

Fig. 2. Schematic depiction of ion transport in a conjugated polymer. To maintain electroneutrality, charges arising during redox reactions are balanced by incorporation or ejection of electrolyte ions into the polymer network, thus, inducing swelling or shrinking of the polymer. Blue arrows denote processes in which the volume increases, black arrows denote decrease in volume. (For interpretation of the references to colour in this figure legend, the reader is referred to the web version of this article.)

If the polymer is reduced (by application of a potential), the positive charge vanishes. However, as the whole material still has to maintain electroneutrality, the incorporated ions have to be either expelled from the network or their charges have to be balanced by incorporation of ions from the environment (i.e., a liquid electrolyte), resulting in a net ion transport in response to an applied electric field [17,32].

Starting from the oxidised and doped state, two different reduction paths are possible as depicted in Fig. 2:

$$P^{x+} \cdot x A^- + x C^+ + x e^- \rightleftharpoons P^0 \cdot x A^- \cdot x C^+ \tag{1}$$

$$P^{x+} \cdot x A^- + x e^- \rightleftharpoons P^0 + x A^- . \tag{2}$$

Here, P denotes the polymer and A^- and C^+ the anion and cation, respectively. Monovalent ions are chosen here for readability. In reality, higher and differing valence numbers are possible.

In path (2), the anions are expelled from the polymer network while in path (1), the anions remain distributed in the polymer and their charges are balanced by uptake of cations from the liquid electrolyte. The latter reaction goes along with a volume increase of the polymer while ejection of ions causes shrinking. Both processes are reversible.

[1] Under actuation, any stress dependence of the ion flux can be considered to be negligible, for discussion of mechanical sensing effects in conjugated polymers see [30].

Which process occurs primarily depends on the mobility of the involved ion species. For large, immobile anions, only reaction path (1) is viable, thus, causing swelling during reduction and shrinking upon subsequent oxidation. If the anions are medium-sized and mobile, both processes may occur simultaneously, further influenced by the applied electric potential and pH. Furthermore, small and mobile ions allow for so-called "salt draining" in which cations and anions bond together to form a neutral salt and diffuse from the polymer, causing contraction. This superposition of multiple mechanisms with opposing effects can result in fluctuating actuator responses as visible for example in the cyclic voltammetry experiments in [33]. Hence, immobilising either the anion or the cation and, thus, having only a single moving species, is usually desirable for actuator applications [17].

In conjugated polymers, transport of multiple ion species and the associated salts with very different mobilities is possible. The different transport paths offer a variety of possible actuation reactions, influenced by the choice of electrolyte and doping ions, making it difficult to predict the superimposed deformation behaviour of the actuator. Therefore, the transport mechanisms and the resulting deformation behaviour are the focus in modelling the composite's behaviour in the following.

3. Mathematical model: Bulk and interface mechanics

The coupling between mechanics, ion transport, and electrostatics has to be considered in order to model actuation in the nanocomposite. These phenomena are described in terms of the evolution of the displacement field $\boldsymbol{u}(\boldsymbol{X}, t)$, the concentration of ion species i $c_0^i(\boldsymbol{X}, t)$, and the electrical potential $\phi(\boldsymbol{X}, t)$.

As described by Wilmers et al. [29], the governing equations are the balance of linear momentum, the balance of mass for the species i and Gauß's law. In the bulk, those read

$$\rho_0 \ddot{\boldsymbol{u}} = \operatorname{Div} \boldsymbol{P} + \rho_0 \boldsymbol{b}\,, \tag{3}$$

$$\dot{c}_0^i = -\operatorname{Div} \boldsymbol{J}^i + W^i\,, \tag{4}$$

$$0 = -\operatorname{Div} \boldsymbol{D} + q_0^f\,, \tag{5}$$

and on the interface, one obtains

$$\overline{\rho}_0 \ddot{\overline{\boldsymbol{u}}} = \overline{\operatorname{Div} \boldsymbol{P}} + \overline{\rho}_0 \overline{\boldsymbol{b}} + [\![\boldsymbol{P}]\!] \cdot \overline{\boldsymbol{N}}\,, \tag{6}$$

$$\dot{\overline{c}}_0^i = -\overline{\operatorname{Div} \boldsymbol{J}^i} + \overline{W}^i - [\![\boldsymbol{J}^i]\!] \cdot \overline{\boldsymbol{N}}\,, \tag{7}$$

$$0 = -\overline{\operatorname{Div} \boldsymbol{D}} + \overline{\operatorname{Div} \boldsymbol{N}} \left[\overline{\boldsymbol{D}} \cdot \overline{\boldsymbol{N}}\right] + \overline{q}_0^f - [\![\boldsymbol{D}]\!] \cdot \overline{\boldsymbol{N}}\,. \tag{8}$$

This system of non-linear equations captures large deformations. Here, the overbar denotes an interface quantity and $[\![\bullet]\!]$ is the jump of a bulk quantity over the interface with $\overline{\boldsymbol{N}}$ being the normal vector to the interface. $\boldsymbol{P}$ is the first Piola–Kirchhoff stress tensor, $\boldsymbol{J}^i$ is the flux of species i and $\boldsymbol{D}$ is the nominal electric displacement field. The sources $\boldsymbol{b}$, W^i and q_0^f are the specific body force tensor, ion sources and the free charge density, respectively. The mass density with respect to the reference configuration is given by ρ_0. As an extension of the surface elasticity theory of Gurtin and Murdoch [34], this model endows the interface with its own thermodynamic structure, resulting in a designated constitutive description for the interface quantities as discussed in the following. For details on the derivation of the interface relations, refer to [29,35].

The composite described here consists of four distinct domains with differing physical behaviour: the polymer, the liquid electrolyte, the nanoporous metal and the interface.

3.1. Metal

The nanoporous metal is considered to be a perfect conductor, thus, no discontinuities in the electron concentration or electric potential arise within the material. Therefore, the system of equations in the metal reduces to the linear momentum balance (Eq. (3)).

The actuation strains in nanoporous metals are fully reversible [36] and its mechanical behaviour is described by the Neo-Hookean model

$$\boldsymbol{P} = \mu \boldsymbol{F} + [\lambda \ln J - \mu] \boldsymbol{F}^{-T}. \tag{9}$$

Here, μ and λ are Lamé parameters, $\boldsymbol{F}$ is the deformation gradient, and J its determinant.

3.2. Polymer

In the bulk polymer, full chemoelectromechanical coupling occurs, i.e., the whole set of governing equations (Eqs. (3)–(5)) has to be solved.

For the stresses, we adopt the constitutive relation of Wilmers et al. [29] in which the first Piola–Kirchhoff stress is additively decomposed into a mechanical and a chemical stress

$$\begin{aligned} \boldsymbol{P} &= \boldsymbol{P}^{\text{mech}} + \boldsymbol{P}^{\text{chem}} \\ &= \mu \boldsymbol{F} + [\lambda \ln J - \mu] \boldsymbol{F}^{-T} - \sum_i k^i F \Delta c_0^i \, \boldsymbol{F}^{-T}, \end{aligned} \tag{10}$$

where the mechanical stress is given by a Neo-Hookean relation. The chemical stress for each species i is proportional to the difference in concentration Δc_0^i at time t to the initial (uncharged) state multiplied with the Faraday constant F. The proportionality constant k^i is a constitutive parameter describing the induced deformation in terms of deformation energy per charge of species i.

In accordance with the results of [29], a possible contribution of the Maxwell stress is negligible. Furthermore, we do not include osmotic effects [27] in the model, as [37] points out that ion insertion dominates actuation in polypyrrole at short time scales while the osmotic pressure dominates at longer times.

The ion flux of species i is modelled by the well-known Nernst–Planck relation (without convection):

$$\boldsymbol{J}^i = -\boldsymbol{D}^i \cdot \operatorname{Grad} c_0^i - c_0^i \frac{z^i F}{RT} \boldsymbol{D}^i \cdot \operatorname{Grad} \phi\,, \tag{11}$$

with the diffusion coefficient $\boldsymbol{D}^i$, the gas constant R and absolute temperature T.

The presence of multiple, differently charged mobile ion species allows for the formation of a neutral salt, compare Fig. 2, according to

$$m A^{n-} + n C^{m+} \underset{r_d}{\overset{r_a}{\rightleftharpoons}} A_m C_n\,. \tag{12}$$

Here, r_a and r_d are the rates of association and dissociation, respectively. Eq. (12) states that m anions and n cations together form one salt molecule in a reversible reaction. In general, the equilibrium state for this reaction lies somewhere inbetween complete dissociation (only ions) and full association (only salt) depending on the rates. This continuous creation and destruction of salt ions is described by the source term W^i in Eq. (4):

$$W^{\text{salt}} = c_{0,\max}^{\text{salt}} \left[r_a \left[\frac{c_0^+}{c_{0,\max}^{\text{salt}}} \right]^n \left[\frac{c_0^-}{c_{0,\max}^{\text{salt}}} \right]^m - r_d \frac{c_0^{\text{salt}}}{c_{0,\max}^{\text{salt}}} \right]. \tag{13}$$

Here, $c_{0,\max}^{\text{salt}}$ denotes the maximum possible salt concentration and is used to normalise the concentrations. The expression $\left[\frac{c_0^+}{c_{0,\max}^{\text{salt}}}\right]^n \left[\frac{c_0^-}{c_{0,\max}^{\text{salt}}}\right]^m$ is the probability of the necessary number of ions "meeting" and, thus, enabling formation of a salt molecule. An increase in salt concentration naturally decreases the concentration of the ions, therefore, $n\,W^+ = m\,W^- = -W^{\text{salt}}$.

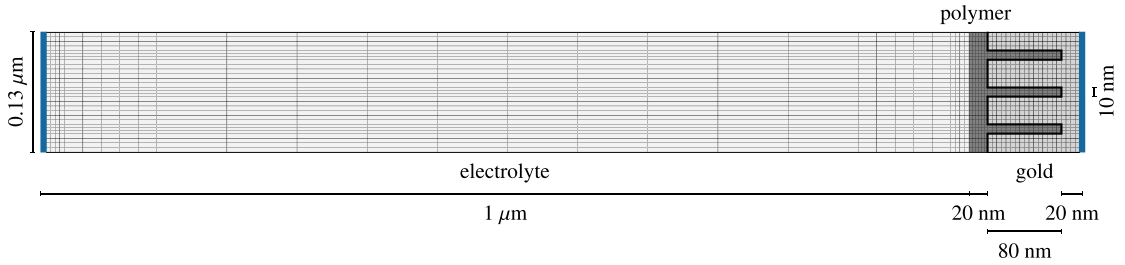

Fig. 3. Meshed geometry of the electric cell with a nanoporous gold–polypyrrole composite electrode. The pore channels in the gold have a diameter of 10 nm and are completely filled with polymer. The electrolyte domain has a width of 1 μm. Boundary conditions on the left-hand side and the interface, are used to apply the potential difference. Displacement of the right-hand side is fully constrained, while all other boundaries are flux- resp. traction-free.

Table 1
Material parameters.

	Symbol	Value
Polymer (polypyrrole)		
Mass density	ρ_0	1.47 g/cm^3 [40]
Lamé parameters	λ	0.346 GPa [41]
	μ	0.231 GPa [41]
Relative permittivity	ε_r	10 000
Valence anion	z^-	-1
Valence cation	z^+	1
Anion concentration	c_0^-	1500 mol/m^3
Cation concentration	c_0^+	0 mol/m^3
Max. salt concentration	$c_{0,\max}^{\text{salt}}$	1500 mol/m^3
Cation diffusivity	D^+	$10 \cdot 10^{-10}$ m^2/s
Coupling parameters	k^-	5 J/C
	k^+	2.5 J/C
	k^{salt}	$0.75[\lvert z^+\rvert k^- + \lvert z^-\rvert k^+]$
Salt association rate	r_a	10 1/ms
Salt dissociation rate	r_d	5 1/ms
Electrolyte		
Relative permittivity	ε_r	8000
Anion concentration	c_0^-	500 mol/m^3
Cation concentration	c_0^+	500 mol/m^3
Anion diffusivity	D^+	$10 \cdot 10^{-10}$ m^2/s
Salt association rate	r_a	0 1/ms
Salt dissociation rate	r_d	100 1/ms
Metal (gold)		
Mass density	ρ_0	19.3 g/cm^3
Lamé parameters	λ	198.6 GPa [42]
	μ	27.08 GPa [42]
Interface		
Lamé parameters	$\overline{\lambda}$	-2 N/m [a]
	$\overline{\mu}$	3.5 N/m [a]
Coupling parameter	$\overline{\xi}^{\text{ion}}$	30 J/C [b]

[a] Based on the surface parameters computed in [43].
[b] Provided by N. Mameka at Helmholtz-Zentrum Geesthacht based on [5].

Salt carries no charge and is, thus, not affected by gradients in the electric potential. Hence, for the salt, Eq. (11) reduces to purely diffusive transport.

Ion transport is significantly slower than electron transport in the polymer and the resistance for ions to cross polymer-solution interface is negligible [38]. Consequently, the electron charge contribution is represented by a homogeneous charge density q_0^p that vanishes over time upon application of a potential.

Thus, the charge density in the polymer is given by:

$$q_0^f(\boldsymbol{X}, t) = F\left[z^+ c_0^+(\boldsymbol{X}, t) + z^- c_0^-(\boldsymbol{X}, t)\right] + q_0^p(t)\,. \tag{14}$$

Here, the valencies and concentrations of the cation and the anion are marked by the superscript $+$ and $-$, respectively.

Finally, the nominal electric displacement is assumed to be homogeneous and electrically linear [29,39], yielding the expression

$$\boldsymbol{D} = -\varepsilon_0 \varepsilon_r J \boldsymbol{F}^{-1} \cdot \boldsymbol{F}^{-T} \cdot \operatorname{Grad} \phi\,, \tag{15}$$

which is the pull-back of the electric displacement field of classical electrostatics to the reference configuration. The electric permittivity of the material is denoted by the product $\varepsilon_0 \varepsilon_r$.

3.3. Liquid electrolyte

The liquid electrolyte does not impose any pressure on the solids and their deformation does not induce any pressure differences in the liquid. Thus, there exists no mechanical interaction between the liquid and the solid domains and the electrolyte behaviour is governed by Eqs. (4) and (5).

The principles of ion transport and salt formation in the liquid are the same as in the polymer. Hence, Eqs. (11) and (12) describe the constitutive behaviour of the electrolyte. Furthermore, the electrolyte exhibits electrically linear behaviour as modelled by Eq. (15).

3.4. Metal/electrolyte interface

The electromechanical coupling on the interface arises from the presence of an interface charge $\overline{q}_0^f$. The stresses induced by this interface charge are modelled with a phenomenological expression introduced in Wilmers et al. [29] utilising the electroelastic coupling parameter $\overline{\xi}^i$ [5]:

$$\begin{aligned}\overline{\boldsymbol{P}} &= \overline{\boldsymbol{P}}^{\text{mech}} + \overline{\boldsymbol{P}}^{\text{electro}} \\ &= \overline{\mu}\overline{\boldsymbol{F}} + \left[\overline{\lambda}\ln\overline{J} - \overline{\mu}\right]\overline{\boldsymbol{F}}^{-T} - \overline{\xi}^i\,\overline{q}_0^f\overline{\boldsymbol{F}}\,.\end{aligned} \tag{16}$$

$\overline{\boldsymbol{F}}$ denotes the deformation gradient on the interface and $\overline{\mu}$ and $\overline{\lambda}$ are the interface Lamé parameters. Here, the mechanically induced stress is described by a Neo-Hookean material model for the interface. Furthermore, the interface is assumed to be geometrically coherent, i.e., there is no displacement discontinuity over the interface, and non-diffusive.

Following the discussion in [29], for the interface of an ideal conductor, the interface electric displacement field vanishes, i.e., $\overline{\boldsymbol{D}} = \boldsymbol{0}$. Therefore, Gauß's law Eq. (8) reduces to the classical interface condition of electrostatics, $0 = \overline{q}_0^f - [\![\boldsymbol{D}]\!] \cdot \overline{\boldsymbol{N}}$, which allows to determine the interface charge from the jump in the electric displacement field over the interface, providing a coupling between bulk and interface behaviour.

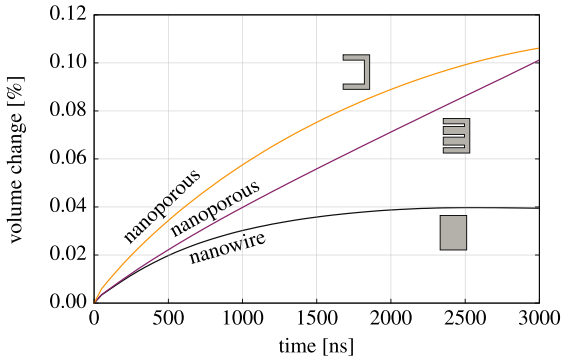

(a) Oxidation.

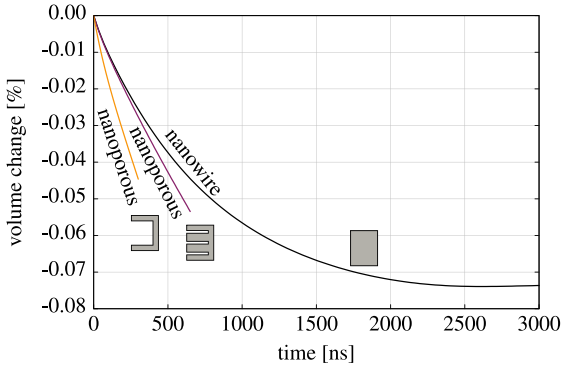

(b) Reduction.

Fig. 4. Volume change of the gold electrode due to actuation in a liquid electrolyte for (a) an oxidising and (b) a reducing potential. The positive (negative) interface charge during oxidation (reduction) results in expansion (compression) of the gold. The largest degree of deformation arises in both cases for large pore diameters, despite the fact that the interface-per-volume ratio is slightly larger for small pore diameters.

4. Numerical results: electric cell

In order to study the influence of different electrode geometries and the presence of a polymer on the actuation behaviour of nanoporous gold, a 2D electric cell as depicted in Fig. 3 is set up. Here, the nanoporous gold's structure is approximated by pore channels in the gold domain. A structure with a single large pore (90 nm pore diameter) and a piece of nanowire with a flat surface are considered for comparison. Complete filling of the pores with polymer and perfect contact are assumed.

A potential difference of ± 0.5 V is applied to the geometry by imposing constant potential boundary conditions on the side of the electrolyte domain and the metal–polymer interface. Displacement of the electrode is constrained on the right-hand (non-electrolyte) side. All other surfaces are flux resp. traction free.

The material parameters for all four domains are listed in Table 1. The transport parameters in the polymer and the electrolyte are chosen not to represent specific anions and cations but so as to illustrate general trends in the nanocomposite behaviour. To allow comparisons between set-ups with and without polymer, the diffusivities in the electrolyte and in the polymer are set to the same value. In reality, diffusivities in the liquid are significantly larger than in the polymer. Further, we utilise slightly exaggerated relative permittivities. The relative permittivity describes the possible size of space charge regions. The smaller the permittivity, the smaller these regions and, consequently, the finer the mesh needs to be, resulting in unreasonably high simulation times. In keeping with the approach utilised in [26], the relative permittivities of the electrolyte and the polymer have been increased to mitigate this effect.

Simulations are carried out using an in-house finite element code utilising the `deal.ii` library [44]. The non-linear system of equations is solved using a monolithic scheme, thus, all coupling effects are accounted for.

4.1. Actuation in liquid electrolyte

To model actuation of pure nanoporous gold in a liquid electrolyte, the polymer domain shown in Fig. 3 (and in the large pore and nanowire geometries) is assigned the electrolyte material behaviour according to Section 3.3 and Table 1.

Fig. 4 compares the initial volume change occurring for the same applied potential difference in the different geometries. The nanowire has the smallest interface length-per-area ratio and, therefore, exhibits the smallest degree of deformation. By introducing nanopores, the interface length-per-area ratio is significantly increased (5 times as large for 90 nm pore, 5.8 times as large for 10 nm), resulting in the expected enhanced volume changes.

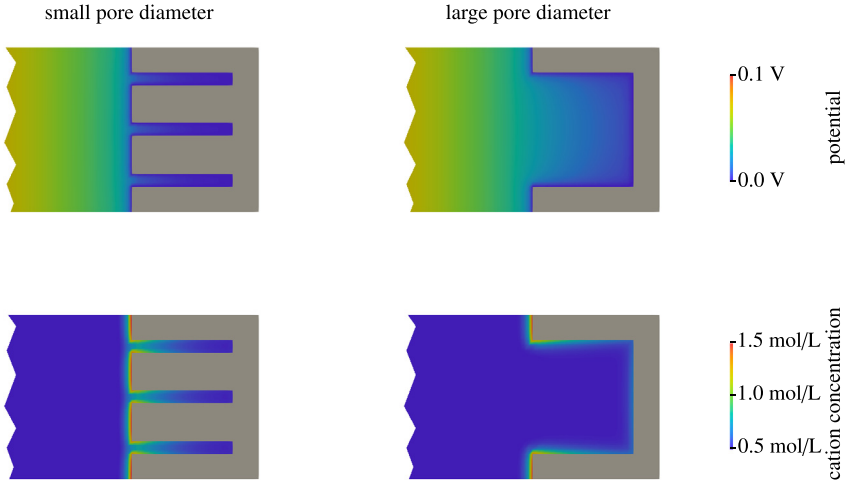

Fig. 5. Effect of the pore diameter on the electric potential and cation concentration distributions under reduction. The large pore geometry allows for potential variation over the pore diameter and, thus, for larger electric fields and surface charges, resulting in increased actuation strains.

However, the relationship between geometry and actuation behaviour especially in the early stages of deformation is more complex than that, as is evident from the fact that the large pore geometry exhibits the largest deformations, despite its interface length-per-area ratio being slightly lower than that of the 10 nm pore geometry. This behaviour is due to the differences in the electric potential distributions over the different pore diameters as depicted in Fig. 5. Comparison of the fields in the two structures reveals that the larger pore diameter allows for potential variation over the pore diameter and, thus, for larger electric fields and surface charges deeper into the pore, resulting in increased actuation strains, as is also evident by the increased countering cation concentration along the interface. Over time, this difference decreases as seen in Fig. 4.

The results demonstrate that not only the interface area is a major influencing factor on the nanocomposite's behaviour but that the pore geometry also strongly affects the actuation response. Here, it is important to note that ever smaller pores (and increased interface areas) might not be advantageous because the pore size affects the electric fields and ion transport behaviour as seen in Fig. 5 and it is necessary to strike a compromise between pore diameter and interface area. With the increasing controllability of synthesis methods, hierarchical nanoporous structures seem to be the answer as they allow to combine different pore geometries in one actuator.

4.2. Actuation in metal–polymer composite

Experiments show that functionalisation of nanoporous gold with polypyrrole results in a significant increase in actuation strain. This effect is also predicted by the model as seen in Fig. 6 which shows the strain over the height of the electrode along the left gold edge. For the case of highly mobile anions, the actuation behaviour in polypyrrole acts in the same direction as the actuation due to the presence of an interface charge, resulting in much larger achievable strains for nanoporous metal composites. For the nanowire, on the other hand, the thin coating with conducting polypyrrole actually reduces the achievable strains because the polymer is free to deform into the electrolyte domain.

The nanoporous structure with small pore diameters profits the most from the presence of the polymer, exhibiting increases in actuation strain of approximately 250% under reduction and over 400% under oxidation. This difference between the two loading cases is a direct result of the choice of the coupling parameter which for anions (which are responsible for the swelling under oxidation) is twice that of the cation.

These results clearly show that the model captures and predicts the influence of the polymer phase on actuation and, thus, offers a unique opportunity to study the effects of other polymer properties, most importantly, the ion mobility.

To examine the effect ion mobilities have on the behaviour of the nanocomposite, four different cases are considered: identical diffusivities of cations and anions (with and without salt drain), fully immobile anions ($D^- = 0$), and cations with increased mobility ($D^+ = 2D^-$). The strain response for the 10 nm pore under reduction is shown in Fig. 7 for these four cases.

For mobile anions, negative actuation strains arise due to anions leaving the polymer network. If salt draining occurs, this effect is enhanced: if the actuator is kept at a certain potential for longer times, the salt also takes cations along when leaving the polymer network. Increased cation mobility ($D^+ > D^-$) results in faster levelling of the actuator's response as cation ingress induces renewed swelling of the polymer. Immobilising the anions, on the other hand, yields steady swelling of the nanocomposite. This response is opposite to the one pure nanoporous gold exhibits but might nevertheless be preferable in many application cases as it prevents

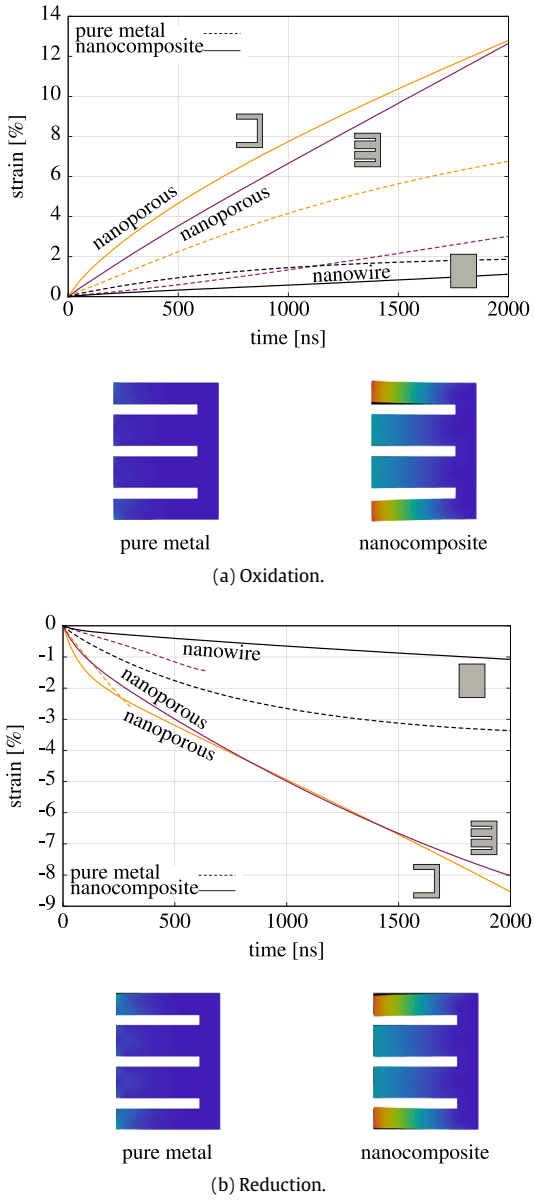

Fig. 6. Actuation strain for different geometries under (a) an oxidising and (b) a reducing potential. Dashed lines are strains in pure metal and solid lines are strains in nanocomposite. The colour plots show the norm of the displacement in one of the nanoporous structures at 500 ns. The nanocomposites exhibit significantly larger strains than the pure metal. For small pore diameters, the influence of the polymer is the most pronounced with an increase in strain of over four times in case of oxidation and over twice as large strains in case of reduction.

changes in the actuation direction over time [17] and effectively prevents salt drain.

The presence of the polymer phase in a nanocomposite actuator not only serves to enhance the actuation strains, but also offers the opportunity to tailor the actuator's behaviour to different specifications by variation of the present ion species and their mobility. For instance, immobilising the anion allows to reverse the actuator's strain direction, and large differences in the anion and cation mobilities result in "switching" responses. As the magnitude of such effects is not easily predicted from experiments because of the complex coupling of the fields, computational modelling as presented in this contribution is an invaluable tool in actuator development.

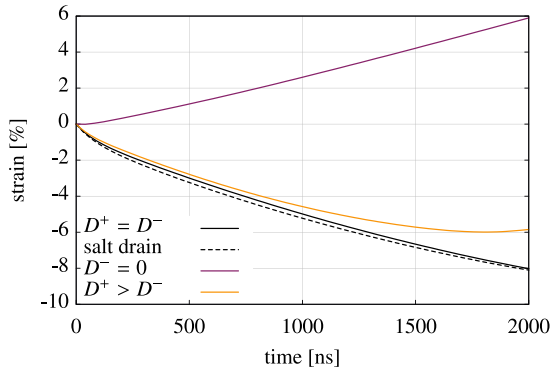

Fig. 7. Strain over time for different ion mobilities. If the anion is immobile ($D^- = 0$), no shrinking occurs, yielding a steady volume increase.

5. Conclusions

Using an interface-extended continuum mechanical framework, the actuation behaviour of nanoporous metal–polymer composites is simulated. Computational modelling of the nanocomposite's response offers insights into material behaviour that is inaccessible to experiments, such as the nature of the superposition of the metal's and the polymer's actuation behaviour and the mechanisms involved in ion transport.

By comparing the responses of pure metal and nanocomposite actuators, a significant increase in actuation strain due to the presence of the polymer phase is found, a behaviour that has also been observed in experiments as well [15,16]. Furthermore, insight into the ion transport mechanism within the polymer and its influence on the actuation is gained, highlighting the strong dependence of the actuator's response on the ion mobilities.

The simulation results show that the increased interface-to-volume ratio of nanoporous metals warrants the attention as base materials for actuators they have received in recent years. However, the results also prove that not only interface area plays a significant role in the actuation behaviour but also geometrical factors such as pore channel diameters, where larger diameters reduce the specific interface area but improve ion transport and electric field distribution. From this point of view, hierarchical nanoporous structures [21,22,45] seem especially promising.

Further attention should be directed to the study of electroactive nanocomposites as the presence of an electroactive polymer is found to drastically improve the actuation behaviour particularly for smaller pore diameters that do not perform as well in a pure metal actuator. As the polymer phase's behaviour is controlled by the mobility of ions in its network, a nanocomposite actuator's response can be tailored to requirements, providing an exciting option for specialised applications requiring "smart" materials.

Acknowledgements

We gratefully acknowledge financial support from the German Research Foundation (DFG) via SFB 986 "M^3", project B6. Furthermore, we would like to thank Jürgen Markmann (Helmholtz-Zentrum Geesthacht, Germany) for fruitful discussions.

References

[1] C. Soyarslan, S. Bargmann, M. Pradas, J. Weissmüller, 3D stochastic bicontinuous microstructures: Generation, topology and elasticity, Acta Mater. 149 (2018) 326–340.
[2] J. Biener, A.M. Hodge, J.R. Hayes, C.A. Volkert, L.A. Zepeda-Ruiz, A.V. Hamza, F.F. Abraham, Size effects on the mechanical behavior of nanoporous Au, Nano Lett. 6 (10) (2006) 2379–2382. PMID: 17034115.
[3] A. Leitner, V. Maier-Kiener, J. Jeong, M. Abad, P. Hosemann, S. Oh, D. Kiener, Interface dominated mechanical properties of ultra-fine grained and nanoporous Au at elevated temperatures, Acta Mater. 121 (2016) 104–116.
[4] H.-J. Jin, J. Weissmüller, Bulk nanoporous metal for actuation, Adv. Energy Mater. 12 (8) (2010) 714–723.
[5] N. Mameka, J. Markmann, H.-J. Jin, J. Weissmüller, Electrical stiffness modulation–confirming the impact of surface excess elasticity on the mechanics of nanomaterials, Acta Mater. 76 (2014) 272–280.
[6] C. Stenner, L.-H. Shao, N. Mameka, J. Weissmüller, Piezoelectric gold: Strong charge-load response in a metal-based hybrid nanomaterial, Adv. Funct. Mater. 26 (28) (2016) 5174–5181.
[7] J. Zhang, Y. Wang, C. Si, Q. Bai, W. Ma, H. Gao, Z. Zhang, Electrochemical actuation behaviors of bulk nanoporous palladium in acid and alkaline solutions, Electrochim. Acta 220 (2016) 91–97.
[8] S. Shi, J. Markmann, J. Weissmüller, Actuation by hydrogen electrosorption in hierarchical nanoporous palladium, Phil. Mag. 97 (19) (2017) 1571–1587.
[9] E. Detsi, M. Sánchez Sellès, P.R. Onck, J.Th.M. De Hosson, Nanoporous silver as electrochemical actuator, Scr. Mater. 69 (2) (2013) 195–198.
[10] L. Yuan, L. Jiang, T. Zhang, G. Wang, S. Wang, X. Bao, G. Sun, Electrochemically synthesized freestanding 3D nanoporous silver electrode with high electrocatalytic activity, Catal. Sci. Technol. 6 (2016) 7163–7171.
[11] I. Okulov, J. Weissmüller, J. Markmann, Dealloying-based interpenetrating-phase nanocomposites matching the elastic behavior of human bone, Sci. Rep. 7 (20) (2017).
[12] M. Hakamada, M. Mabuchi, Nanoporous nickel fabricated by dealloying of rolled Ni-Mn sheet, Procedia Eng. 81 (2014) 2159–2164. 11th International Conference on Technology of Plasticity, ICTP 2014, 19–24 October 2014, Nagoya Congress Center, Nagoya, Japan.
[13] Q. Lu, G.S. Hutchings, W. Yu, Y. Zhou, R.V. Forest, R. Tao, J. Rosen, B.T. Yonemoto, Z. Cao, H. Zheng, et al., Highly porous non-precious bimetallic electrocatalysts for efficient hydrogen evolution, Nature Commun. 6 (2015).
[14] J. Zhang, L. Lv, H. Gao, Q. Bai, C. Zhang, Z. Zhang, Electrochemical actuation behaviors and mechanisms of bulk nanoporous Ni-Pd alloy, Scr. Mater. 137 (2017) 73–77.
[15] E. Detsi, P. Onck, J. De Hosson, Metallic muscles at work: High rate actuation in nanoporous gold/polyaniline composites, ACS Nano 7 (5) (2013) 4299–4306.
[16] K. Wang, C. Stenner, J. Weissmüller, A nanoporous gold-polypyrrole hybrid nanomaterial for actuation, Sensors Actuators B 248 (2017) 622–629.
[17] E. Smela, Conjugated polymer actuators for biomedical applications, Adv. Mater. 15 (2003) 481–494.
[18] E. Griffiths, S. Bargmann, B.D. Reddy, Elastic behaviour at the nanoscale of innovative composites of nanoporous gold and polymer, Extreme Mech. Lett. 17 (2017) 16–23.
[19] S. Bargmann, C. Soyarslan, E. Husser, N. Konchakova, Materials based design of structures: Computational modeling of the mechanical behavior of gold-polymer nanocomposites, Mech. Mater. 94 (2016) 53–65.
[20] K. Wang, J. Weissmüller, Composites of nanoporous gold and polymer, Adv. Mater. 25 (9) (2013) 1280–1284.
[21] T. Fujita, Y. Kanoko, Y. Ito, L. Chen, A. Hirata, H. Kashani, O. Iwatsu, M. Chen, Nanoporous metal papers for scalable hierarchical electrode, Adv. Sci. 2 (8) (2015) 1500086.
[22] T. Juarez, J. Biener, J. Weissmüller, A.M. Hodge, Nanoporous metals with structural hierarchy: A review, Adv. Energy Mater. (2017) 1700389.
[23] S. Nemat-Nasser, Micromechanics of actuation of ionic polymer-metal composites, J. Appl. Phys. 92 (5) (2002) 2899–2915.
[24] P. Nardinocchi, M. Pezzulla, L. Placidi, Thermodynamically based multiphysic modeling of ionic polymer metal composites, J. Intell. Mater. Syst. Struct. 22 (16) (2011) 1887–1897.
[25] Y. Cha, M. Porfiri, Mechanics and electrochemistry of ionic polymer metal composites, J. Mech. Phys. Solids 71 (2014) 156–178.
[26] X. Wang, B. Shapiro, E. Smela, Development of a model for charge transport in conjugated polymers, J. Phys. Chem. C 113 (1) (2009) 382–401.
[27] L. Bay, T. Jacobsen, S. Skaarup, K. West, Mechanism of actuation in conducting polymers: Osmotic expansion, J. Phys. Chem. B 105 (36) (2001) 8492–8497.
[28] V. Venugopal, H. Zhang, R. Northcutt, V.B. Sundaresan, A thermodynamic chemomechanical constitutive model for conducting polymers, Sensors Actuators B 201 (2014) 293–299.
[29] J. Wilmers, A. McBride, S. Bargmann, Interface elasticity effects in polymer-filled nanoporous metals, J. Mech. Phys. Solids 99 (2017) 163–177.
[30] Y. Wu, G. Alici, J.D.W. Madden, G.M. Spinks, G.G. Wallace, Soft mechanical sensors through reverse actuation in polypyrrole, Adv. Funct. Mater. 17 (16) (2007) 3216–3222.
[31] T.V. Vernitskaya, O.N. Efimov, Polypyrrole: a conducting polymer; its synthesis, properties and applications, Russ. Chem. Rev. 66 (5) (1997) 443.
[32] E.W.H. Jager, E. Smela, O. Inganäs, Microfabricating conjugated polymer actuators, Science 290 (5496) (2000) 1540–1545.
[33] M.R. Gandhi, P. Murray, G.M. Spinks, G.G. Wallace, Mechanism of electromechanical actuation in polypyrrole, Synth. Met. 73 (3) (1995) 247–256.

[34] M.E. Gurtin, A.I. Murdoch, A continuum theory of elastic material surfaces, Arch. Ration. Mech. Anal. (ISSN: 1432-0673) 57 (4) (1975) 291–323. http://dx.doi.org/10.1007/BF00261375.
[35] A.T. McBride, A. Javili, P. Steinmann, S. Bargmann, Geometrically nonlinear continuum thermomechanics with surface energies coupled to diffusion, J. Mech. Phys. Solids 59 (10) (2011) 2116–2133.
[36] J. Weissmüller, R.N. Viswanath, D. Kramer, P. Zimmer, R. Würschum, H. Gleiter, Charge-Induced reversible strain in a metal, Science 300 (5617) (2003) 312–315.
[37] J.G. Martinez, T.F. Otero, E.W.H. Jager, Effect of the electrolyte concentration and substrate on conducting polymer actuators, Langmuir 30 (13) (2014) 3894–3904. PMID: 24605916.
[38] T. Komura, S. Goisihara, T. Yamaguti, K. Takahasi, Electron and ion transport in polypyrrole/polystyrenesulfonate composite films, J. Electrochem. Soc. 456 (1–2) (1998) 121–129.
[39] A.L. Dorfmann, R.W. Ogden, Nonlinear theory of electroelastic and magnetoelastic interactions, Springer US, 2014.
[40] J.J. López Cascales, T.F. Otero, Molecular dynamic simulation of the hydration and diffusion of chloride ions from bulk water to polypyrrole matrix, J. Chem. Phys. 120 (4) (2004) 1951–1957.
[41] J. Foroughi, S.R. Ghorbani, G. Peleckis, G.M. Spinks, G.G. Wallace, X.L. Wang, S.X. Dou, The mechanical and the electrical properties of conducting polypyrrole fibers, J. Appl. Phys. 107 (10) (2010).
[42] T.J. Balk, C. Eberl, Y. Sun, K.J. Hemker, D.S. Gianola, Tensile and compressive microspecimen testing of bulk nanoporous gold, JOM 61 (12) (2009) 26–31.
[43] B. Elsner, S. Müller, S. Bargmann, J. Weissmüller, Surface excess elasticity of gold: Ab initio coefficients and impact on the effective elastic response of nanowires, Acta Mater. 124 (2017) 468–477.
[44] W. Bangerth, R. Hartmann, G. Kanschat, deal.II –a general purpose object oriented finite element library, ACM Trans. Math. Software 33 (4) (2007) 24/1–24/27.
[45] S. Bargmann, B. Klusemann, J. Markmann, J. Schnabel, K. Schneider, C. Soyarslan, J. Wilmers, Generation of 3d representative volume elements (RVEs) for heterogeneous materials: a review, Prog. Mater. Sci. (2018). http://dx.doi.org/10.1016/j.pmatsci.2018.02.003.